

An antenna-coupled bolometer with an integrated microstrip bandpass filter

Michael J. Myers,^{a)} William Holzapfel, Adrian T. Lee, Roger O'Brient, P. L. Richards, and Huan T. Tran
Department of Physics, University of California, Berkeley, California, 94720

Peter Ade
School of Physics and Astronomy, Cardiff University, Cardiff, Wales, United Kingdom

Greg Engargiola
Department of Astronomy, University of California, Berkeley, California 94720

Andy Smith
Northrop Grumman, Redondo Beach, California 90278

Helmuth Spieler
Lawrence Berkeley National Laboratory, Berkeley, California 94720

(Received 17 September 2004; accepted 17 January 2005; published online 8 March 2005)

We describe the fabrication and testing of antenna-coupled superconducting transition-edge bolometers for use at millimeter wavelengths. The design uses a double-slot dipole antenna connected to superconducting niobium microstrip. Band defining filters are implemented in the microstrip, which is then terminated with a load resistor. The power dissipated in the load resistor is measured by a superconducting transition-edge sensor (TES). The load resistor and TES are thermally well connected and are supported by a silicon nitride substrate. The substrate is suspended by four narrow silicon nitride legs for thermal isolation. The bolometers have been optically characterized and the spectral response is presented. This detector is a prototype element for use in an array designed for studies of the cosmic microwave background polarization. © 2005 American Institute of Physics. [DOI: 10.1063/1.1879115]

Bolometers are the most sensitive broadband detectors of millimeter wavelength radiation. They have been used with great success in observations of the cosmic microwave background (CMB) temperature anisotropy. In this application, single bolometers have already reached the limit in sensitivity set by the statistical arrival of background photons. Arrays of detectors are therefore employed to increase overall sensitivity, with current instruments operating at these wavelengths using 10–100 bolometers. Because the CMB polarization anisotropy is more than an order of magnitude weaker than the temperature anisotropy, arrays of 10^3 – 10^4 or more pixels are needed to characterize the CMB polarization.

Conventional millimeter wavelength photometers use a horn antenna to couple the incident radiation into an absorbing film on a bolometer. Antenna-coupled bolometers^{1–4} use a planar antenna to couple the radiation into a transmission line, which is then terminated by a load resistor. This approach integrates several optical elements onto the detector chip, facilitating the use of large bolometer arrays. The antenna defines an optical beam which can be efficiently coupled to the telescope, eliminating bulky and expensive feed horns. On-chip band defining filters can be constructed as part of the transmission line feeding the antenna in place of the stand-alone quasi-optical filters typically used. Planar antennas are typically sensitive to polarization, which is another advantage in applications where polarization information is useful. Another powerful feature of planar antenna-coupled bolometers is the potential for multicolor pixels on a

single chip. The signal from a broadband antenna can be divided into several bands and read out using separate bolometers. This configuration would provide the most efficient use of focal plane space. Future bolometer arrays will push the achievable field-of-view of millimeter wave telescopes. Therefore, this gain in efficiency will be required to obtain the maximum sensitivity for a large multicolor array.

We have designed and fabricated antenna-coupled bolometers with on-chip band defining filters as prototype pixels for a large bolometer array. Figure 1 is a photograph of the bolometer chip. Our design uses a double-slot dipole antenna⁵ which is resonant at 217 GHz. This antenna has a nearly symmetric beam and a dual-polarized version has been demonstrated.⁶ A silicon hyperhemispherical lens⁵ is used to provide a better match to typical telescope optics and to suppress substrate modes. This lens/antenna combination has been used successfully in applications such as coupling radiation into SIS mixers.⁷

The antenna feeds niobium microstrip with a silicon dioxide dielectric. Niobium microstrip can be very low loss below 700 GHz.⁸ The microstrip impedance is 30Ω at the antenna for optimal impedance matching. A tapered microstrip transformer⁹ is then used to bring the microstrip to a wider 10Ω line. This minimizes the effect of small variations in line width caused by errors in the fabrication process.

We use microstrip filters to define the frequency band over which the bolometer is sensitive. We chose a well known bandpass filter topology using quarter wavelength shorted stubs¹⁰ due to its conceptual simplicity and because the required microstrip impedances were easily realizable

^{a)}Electronic mail: mmyers@cosmology.berkeley.edu

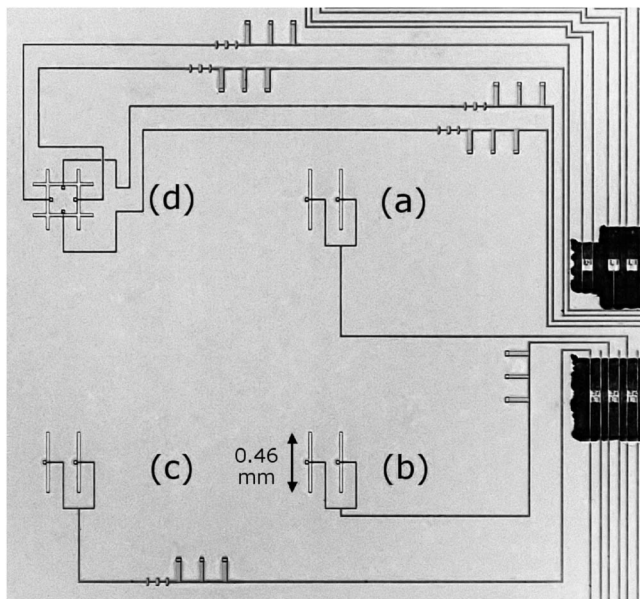


FIG. 1. Image of an antenna-coupled bolometer chip with four test pixels. Labels indicate pixels with (a) no microstrip filters, (b) a microstrip bandpass filter, (c) microstrip bandpass and lowpass filters, and (d) dual polarization antenna and microstrip bandpass and lowpass filters (not tested). The dark area on the right is the region in which silicon was removed to suspend the bolometers.

given our fabrication process. This filter design has a well defined passband, but the periodicity of the resonant structure creates unwanted passbands at odd integer multiples of the design frequency. A stepped-impedance lowpass filter¹⁰ is used to remove the higher frequency bands.

The filters were initially modeled as idealized transmission line elements in MMICAD,¹¹ which is a linear transmission line circuit simulator. The actual microstrip geometry for the filter elements was generated using these results and published models of superconducting microstrip.¹² The performance of the microstrip filters was then verified in Sonnet,¹³ which is a full wave electromagnetic simulator. The effect of the niobium's superconductivity was included in Sonnet as a surface impedance.¹⁴ Excellent agreement was seen between the full wave simulation and the simpler linear model, indicating that the microstrip filter elements behave as nearly ideal transmission lines.

The microstrip is terminated with a load resistor in good thermal contact with a superconducting transition-edge sensor (TES). The TES, which is made of an aluminum/titanium bilayer, measures the power dissipated in the resistor. The T_C of the bilayer is easily tunable over the range of 400–600 mK by varying the relative thicknesses of the metals. This range of T_C is optimal for use with a ³He sorption cooler. For convenience, the load resistor is made from the same material as the TES. Since the photons propagating along the microstrip are of much higher energy than the gap energy of the bilayer, the material acts as a normal metal. The load resistor and TES are located on a leg isolated silicon nitride substrate. This structure provides the thermal isolation needed for the required sensitivity.

The test devices were fabricated in the UC Berkeley Microfab in a monolithic process using standard microfabrication techniques. A 1 μm layer of low stress silicon nitride was deposited on a 100 mm silicon wafer using low pressure chemical vapor deposition. A 0.3 μm layer of niobium was

sputter deposited to form a ground plane. The niobium was patterned to form the slot antenna using a 10:1 reduction wafer stepper, which was used for all lithography steps. The layer was etched using a reactive ion etch (RIE) system and a CF_4 based plasma. A 0.5 μm SiO_2 dielectric layer was deposited in a plasma enhanced chemical vapor deposition system. It was patterned and etched in the same RIE system using a different etch recipe. A 0.6 μm niobium layer was deposited, patterned, and etched as before to create the microstrip layer and the bias lines for the TES.

A 40 nm aluminum/80 nm titanium bilayer was deposited in a single vacuum step to form the TES and the resistor which terminates the microstrip. A sputter etch was necessary immediately before deposition to remove the native niobium oxide. The patterned bilayer was etched using a SF_6 plasma to remove the titanium, followed by a commercial wet aluminum etch. The aluminum etch does not attack the niobium or SiO_2 beneath the bilayer. With the electrical components complete, the silicon nitride suspensions were patterned. The silicon nitride was etched using a SF_6 plasma and the wafer was diced. Individual chips were placed in a gaseous XeF_2 to etch the exposed silicon, suspending the nitride. An O_2 plasma was used to strip the final layer of photoresist.

The devices were tested in a cryostat equipped with a ³He sorption cooler to achieve a 295 mK base temperature. Light was admitted to the dewar through a Zotefoam PPA-30¹⁵ window. A metal mesh filter and an alkali halide filter blocked light above 540 GHz and a 1.3% neutral density filter prevented 300 K radiation from saturating the device. A TPX plastic lens reimaged the detector focus at the window, minimizing the required size of the window and filters. A room temperature current source and a cold 20 m Ω shunt resistor were used to voltage bias the detector. A Quantum Design SQUID current amplifier and model 550 controller were used to measure the current.

Several devices were electrically tested and found to operate as expected. Typical device parameters were a thermal conductance $G=9 \times 10^{-10}$ W/K and a transition temperature $T_C=450$ mK. The optical time constant was $\tau_{\text{opt}} < 0.4$ ms, too small to measure with available optical choppers. The load resistor could not be directly measured in the circuit. An identical test structure had a resistance of 25 Ω , significantly higher than the 10 Ω needed for an optimal match. Simulations show that this should result in a decrease in efficiency of 30%. The deviation was caused by undercutting during the aluminum etch, which can be corrected in future devices. The bolometer noise was not measurable in the optical test system due to poor matching to the Quantum Design SQUID. Similar devices fabricated using the same process have shown the expected white current noise due to thermal fluctuations from below 1 Hz to 100 Hz. For the reported devices, the expected noise equivalent power is $\sim 10^{-16}$ W/ $\sqrt{\text{Hz}}$.

A Fourier transform spectrometer (FTS) was used to measure the spectral response of the receiver. A detector with no microstrip filters showed the expected response peak at the resonant frequency of the antenna. Fringing in the spectrum was seen with a spacing and peak to trough ratio consistent with the expected standing waves on the microstrip line caused by the known impedance mismatch at the load resistor.

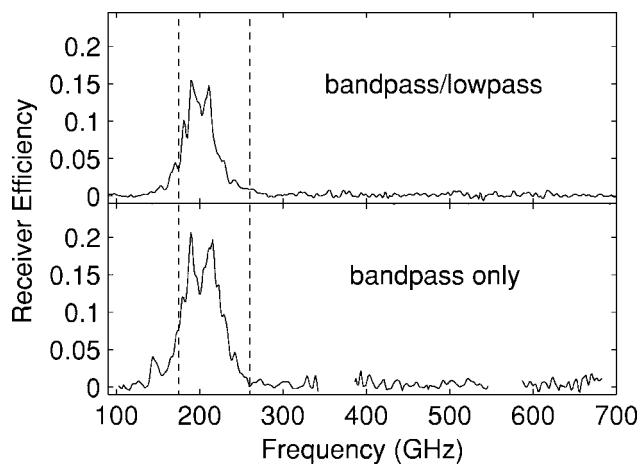


FIG. 2. Measured receiver efficiency for two antenna-coupled bolometers with microstrip filters. Top: device with microstrip bandpass and lowpass filters. Bottom: device with microstrip bandpass filter. The dashed lines show the simulated half power bandwidth for the filters. Missing data in the lower spectrum are due to the FTS beamsplitter nulls.

Devices with microstrip filters were also tested with the FTS. A separate test using a chopped liquid nitrogen load permitted normalization of the spectra to the absolute receiver efficiency. Figure 2 shows that a well defined bandpass response was seen as expected. The unwanted third harmonic passband in the detector with only a microstrip bandpass filter was not visible due to the 540 GHz metal-mesh blocking filter at the entrance to the receiver. In this configuration the on-chip lowpass filter is not necessary. However, it would be required in a multichroic system where the ratio of the highest to lowest frequencies is three or more.

Figure 2 also shows that the measured bands for both detectors were narrower than the design bandwidth. This may be due to incomplete knowledge of the microstrip properties. Measurements of the actual material properties should improve our understanding of the observed detector response. However, the detector response was close enough to simulation that empirical modification of the filter elements may be adequate to achieve the desired performance.

We calculate a theoretical peak receiver efficiency of 25%, which includes the effect of losses in the optics as well as those on the detector chip. As seen in Figure 2, the measured efficiency is somewhat lower than this, especially in the device with a lowpass filter. This may be due to imperfect alignment of the test optics or higher than expected loss in the microstrip. Further work is needed to understand the

source of the discrepancy. The theoretical receiver efficiency can be increased by a factor of two by applying an antireflection coating to the silicon lens and correcting the mismatched load resistor. With the currently demonstrated performance, these two corrections would result in a receiver efficiency competitive with typical systems in use.

The test pixel design will be used as the basis for a bolometer array for a ground based CMB polarization experiment. Since each pixel has a single band, a heterogeneous array will be used to observe in multiple frequency bands. Pixels for different bands can be constructed by simply geometrically scaling the antenna and filters. The design uses a “fly’s eye” lens array,¹⁶ providing a silicon lens for each antenna. Individual silicon lenses can be antireflection coated as in the single pixel case.

The authors thank Xiaofan Meng for significant assistance in the fabrication of the devices described here. All devices were fabricated in the UC Berkeley Microlab. This work is supported by NSF Grant No. AST-0096933. A.T.L. and H.S. are supported by the Director, Office of Science, Office of High Energy and Nuclear Physics, of the U.S. Department of Energy under Contract No. DE-AC03-76SF00098. H.T.T. is supported by the Miller Institute.

¹M. Nahum and P. L. Richards, *IEEE Trans. Magn.* **27**, 2484 (1991).

²J. Mees, M. Nahum, and P. L. Richards, *Appl. Phys. Lett.* **59**, 2329 (1991).

³C. L. Hunt, Ph.D. thesis, California Institute of Technology, 2003.

⁴M. J. Myers, W. Holzappel, A. T. Lee, R. O’Brien, P. L. Richards, D. Schwan, A. D. Smith, H. Spieler, and H. Tran, *Nucl. Instrum. Methods Phys. Res. A* **520**, 424 (2004).

⁵D. Filipovic, S. Gearhart, and G. Rebeiz, *IEEE Trans. Microwave Theory Tech.* **41**, 1738 (1993).

⁶G. Chattopadhyay and J. Zmuidzinas, *IEEE Trans. Antennas Propag.* **46**, 736 (1998).

⁷J. Zmuidzinas, N. G. Ugras, D. Miller, M. Gaidis, H. G. LeDuc, and J. A. Stern, *IEEE Trans. Appl. Supercond.* **5**, 3053 (1995).

⁸R. L. Kautz, *J. Appl. Phys.* **49**, 308 (1978).

⁹D. P. McGinnis and J. B. Beyer, *IEEE Trans. Microwave Theory Tech.* **36**, 1521 (1988).

¹⁰G. Matthaei, L. Young, and E. M. T. Jones, *Microwave Filters, Impedance Matching Networks, and Coupling Structures* (McGraw-Hill, New York, 1964).

¹¹Optotek Ltd., URL <http://www.optotek.com>.

¹²G. Yassin and S. Withington, *J. Phys. D* **28**, 1983 (1995).

¹³Sonnet Software, Inc., URL <http://www.sonnetsoftware.com>.

¹⁴A. R. Kerr, ALMA Memo Series 245 (1999).

¹⁵Zotefoams Inc., URL <http://www.zotefoams-usa.com>.

¹⁶T. H. Buttgenbach, *IEEE Trans. Microwave Theory Tech.* **41**, 1750 (1993).